A&A 478, 163–174 (2008)
DOI: 10.1051/0004-6361:20077775
© ESO 2008

Astronomy & Astrophysics

Stochastic excitation of non-radial modes

I. High-angular-degree *p* modes

K. Belkacem, R. Samadi, M.-J. Goupil, and M.-A. Dupret

Observatoire de Paris, LESIA, CNRS UMR 8109, 92190 Meudon, France
e-mail: Kevin.Belkacem@obspm.fr

Received 2 May 2007 / Accepted 3 October 2007

ABSTRACT

Context. Turbulent motions in stellar convection zones generate acoustic energy, part of which is then supplied to normal modes of the star. Their amplitudes result from a balance between the efficiencies of excitation and damping processes in the convection zones.
Aims. We develop a formalism that provides the excitation rates of non-radial global modes excited by turbulent convection. As a first application, we estimated the impact of non-radial effects on excitation rates and amplitudes of the high-angular-degree modes that are observed on the Sun.
Methods. A model of stochastic excitation by turbulent convection was developed to compute the excitation rates and then successfully applied to solar radial modes. We generalise this approach to the case of non-radial global modes. This enables us to estimate the energy supplied to high-(ℓ) acoustic modes. Qualitative arguments, as well as numerical calculations, are used to illustrate the results.
Results. We find that non-radial effects for p modes are non-negligible:
- For high-n modes (i.e. typically $n > 3$) and for high values of ℓ, the power supplied to the oscillations depends on the mode inertia.
- For low-n modes, independent of the value of ℓ, the excitation is dominated by the non-radial components of the Reynolds stress term.
Conclusions. Our numerical investigation of high-ℓ p modes shows that the validity of the present formalism is limited to $\ell < 500$ due to the spatial separation of scale assumption. Thus, a model for very high-ℓ p-mode excitation rates calls for further theoretical developments; however, the formalism is valid for solar g modes, which will be investigated in a paper in preparation.

Key words. convection – turbulence – Sun: oscillations

1. Introduction

Amplitudes of solar-like oscillations result from a balance between stochastic excitation and damping in the outermost layers of the convection zone, which extends nearly to the surface of the star. Accurate measurements of the rate at which acoustic energy is supplied to the solar p modes are available from ground-based observations (GONG, BiSON), as well as from spacecraft (SOHO/GOLF and MDI). From those measurements and a comparison with theoretical models, it has been possible to demonstrate that excitation is due to eddy motions in the uppermost part of the convection zone and by advection of entropy fluctuations.

Stochastic excitation of *radial* modes by turbulent convection has been investigated by means of several semi-analytical approaches (Goldreich & Keeley 1977; Goldreich et al. 1994; Balmforth 1992; Samadi & Goupil 2001), they differ from each other in the nature of the assumed excitation sources, the assumed simplifications and approximations, and also by the way the turbulent convection is described (see reviews by Stein et al. 2004; Houdek 2006). Two major mechanisms have nevertheless been identified as driving the resonant p modes of the stellar cavity: the first is related to the Reynolds stress tensor and, as such, represents a mechanical source of excitation; the second is caused by the advection of turbulent fluctuations of entropy by turbulent motions (the entropy source term), and as such it represents a thermal source of excitation (Goldreich et al. 1994; Stein & Nordlund 2001). Samadi & Goupil (2001, hereafter Paper I) proposed a generalised formalism, taking the Reynolds and entropy fluctuation source terms into account. In this model, the source terms are written as functions of the turbulent kinetic energy spectrum and the temporal-correlation function. This allowed us to investigate several possible models of turbulence (Samadi et al. 2003a,b). The results were compared with GOLF data for radial modes, and the theoretical values were found to be in good agreement with the observations (Samadi et al. 2003b). Part of the remaining discrepancies has recently been removed by taking into account the asymmetry introduced by turbulent plumes (Belkacem et al. 2006a,b).

In this paper we take an additional step by extending the Samadi & Goupil (2001) formalism to the case of non-radial global modes. This will enable us to estimate the excitation rates for a wide variety of p and g modes excited in different types of stars. The present model provides the energy supplied to the modes by turbulence in inner, as well as outer, stellar convective regions, provided the turbulent model appropriate for the relevant region is used. Studies of the stochastic excitation of solar radial modes (Samadi et al. 2003a,b) have given us access mainly to the radial properties of turbulence. The present generalised formalism enables us to take the horizontal properties of turbulence into account (through the non-radial components of the Reynolds stress contribution) in the outermost part of the convective zone.

In the Sun, high-angular-degree p modes (as high as one thousand) have been detected (e.g., Korzennik et al. 2004). From an observational point of view, Woodard et al. (2001) found that the energy supplied to the mode increases with ℓ, but that above

Article published by EDP Sciences and available at http://www.aanda.org or http://dx.doi.org/10.1051/0004-6361:20077775

some high-ℓ value, which depends on the radial order n (see Woodard et al. 2001, Fig. 2), the energy decreases with increasing ℓ. They mention the possibility of an unmodelled mechanism of damping. Hence one of the motivations of this work is to investigate such an issue. As a first step, we develop here a theoretical model of the stochastic excitation taking the ℓ-dependence of the source terms into account to seek a physical meaning for such a behaviour of the amplitudes.

Modelling of the mechanisms responsible for excitating non-radial modes is useful not only for high-ℓ acoustic modes but also for gravity modes, which are intrinsically non-radial. As for p modes, g modes are stochastically excited by turbulent convection; the main difference is that the dominant restoring force for g modes is buoyancy. We, however, stress that convective penetration is another possible excitation mechanism for g modes (e.g. Dintrans et al. 2005). Such modes are trapped in the radiative interior of the Sun, so their detection promises closer knowledge of the deep solar interior. However, they are evanescent in the convection zone; thus, their amplitudes at the surface are very small and their detection remains controversial. A theoretical prediction of their amplitudes is thus an important issue. It requires an estimation of the excitation rates but also of the damping rates. Unlike p modes, the damping rates cannot be inferred from observations, and this introduces considerable uncertainties; e.g., theoretical estimates of the g-mode amplitudes (Gough 1985; Kumar et al. 1996) differ from each other by orders of magnitudes, as pointed out by Christensen-Dalsgaard (2002). We thus stress that the present work focuses on the excitation rates – damping rates are not investigated. A specific study of gravity modes will be considered in a forthcoming paper.

The paper is organised as follows: Sect. 2 introduces the general formalism, and a detailed derivation of the Reynolds and entropy source terms is provided. In Sect. 3, we demonstrate that the formalism of Samadi & Goupil (2001) is a special case and an asymptotic limit of the present model. In Sect. 4, we use qualitative arguments to determine the different contributions to the excitation rates and identify the dominant terms involving the angular degree (ℓ). Section 5 presents the numerical results where excitation rates are presented. Section 6 discusses the limitations of the model and some conclusions are formulated in Sect. 7.

2. General formulation

Following Paper I, we start from the perturbed momentum and continuity equation

$$\frac{\partial(\rho_0+\rho_1)\boldsymbol{v}}{\partial t} + \nabla : (\rho_0 \boldsymbol{v}\boldsymbol{v}) = -\nabla p_1 + \rho_1 \boldsymbol{g}_0 + \rho_0 \boldsymbol{g}_1 + \rho_1 \boldsymbol{g}_1, \tag{1}$$

$$\frac{\partial \rho_1}{\partial t} + \nabla \cdot ((\rho_0+\rho_1)\boldsymbol{v}) = 0 \tag{2}$$

where ρ is the density, p the pressure, and $\boldsymbol{g}$ the gravity. The subscripts 1 and 0 denote Eulerian perturbations and equilibrium quantities, respectively, except for velocity where the subscript 1 has been dropped for ease of notation. In the following, the velocity field is split into two contributions, namely the oscillation velocity ($\boldsymbol{v}_{\rm osc}$) and the turbulent velocity field ($\boldsymbol{u}$), such that $\boldsymbol{v} = \boldsymbol{v}_{\rm osc} + \boldsymbol{u}$. For a given mode, the fluid displacement can be written as

$$\boldsymbol{\delta r}_{\rm osc} = \frac{1}{2}\left(A(t)\,\boldsymbol{\xi}(\boldsymbol{r}) e^{-i\omega_0 t} + c.c.\right), \tag{3}$$

where ω_0 is the eigenfrequency, $\boldsymbol{\xi}(\boldsymbol{r})$ the displacement eigenfunction in the absence of turbulence, $A(t)$ the amplitude due to the turbulent forcing, and $c.c$ denotes the complex conjugate. The power (P) injected into the modes is related to the mean-squared amplitude ($\langle |A|^2 \rangle$) by (see Paper I)

$$P = \eta \langle |A|^2 \rangle I\, \omega_0^2, \tag{4}$$

where the operator $\langle\rangle$ denotes a statistical average performed on an infinite number of independent realisations, η is the damping rate, and I is the mode inertia.

We use the temporal WKB assumption, i.e. that $A(t)$ is slowly varying with respect to the oscillation period, $\eta \approx {\rm d}\ln A(t)/{\rm d}t \ll \omega_0$ (see Paper I for details). Under this assumption, using Eq. (3) with Eqs. (1) and (2) (see Paper I) yields:

$$\frac{{\rm d}A(t)}{{\rm d}t} + \eta A(t) = \frac{1}{2\omega_0^2 I}\int {\rm d}^3x\, \boldsymbol{\xi}^* \cdot \frac{\partial \boldsymbol{S}}{\partial t} e^{i\omega_0 t}, \tag{5}$$

where ${\rm d}^3x$ is the volume element and $\boldsymbol{S} = -(\boldsymbol{f}_t + \boldsymbol{\nabla} h_t + \boldsymbol{g}_t)$ the excitation source terms. Temporal derivatives appearing in Eq. (5) are

- The Reynolds stress contribution

$$\frac{\partial f_t}{\partial t} = -\frac{\partial}{\partial t}\left(\nabla : (\rho_0 \boldsymbol{u}\boldsymbol{u})\right), \tag{6}$$

  where $\boldsymbol{u}$ is the turbulent component of the velocity field.
- The entropy term

$$\frac{\partial}{\partial t}\nabla h_t = -\nabla\left(\alpha_{\rm s}\frac{{\rm d}\delta s_t}{{\rm d}t} - \alpha_{\rm s}\boldsymbol{u}\cdot\nabla \boldsymbol{s}_t\right), \tag{7}$$

  where δs_t is the turbulent Lagrangian fluctuation of the entropy ($\alpha_{\rm s} = {\rm d}p_1/{\rm d}s_t$) and p_1 denotes the Eulerian pressure fluctuations.
  The last term in the right hand side of Eq. (7) represents the advection of entropy fluctuations by turbulent motion and, as such, is a thermal driving. Note that it was shown in Belkacem et al. (2006b) that this term is needed to reproduce the maximum in the amplitude as a function of frequency in the case of solar radial p modes.
- The fluctuating gravity term

$$\frac{\partial g_t}{\partial t} = \frac{\partial \rho_1 g_1}{\partial t}, \tag{8}$$

  where g_1 is the fluctuation of gravity due to the turbulent field. This contribution can be shown to be negligible and will not be considered in detail here for p modes.

Several other excitation source terms appear on the right hand side of Eq. (1). However, as shown in Paper I, their contributions are negligible since they are linear in terms of turbulent fluctuations.[1]

From Eq. (5), one obtains the mean-squared amplitude

$$\begin{aligned}\langle |A|^2(t)\rangle \;=\; & \frac{e^{-2\eta t}}{4(\omega_0 I)^2}\int_{-\infty}^{t} {\rm d}t_1 {\rm d}t_2 \\ & \times \int {\rm d}^3 r_1 {\rm d}^3 r_2 e^{\eta(t_1+t_2)+i\omega_0(t_1-t_2)} \\ & \times \langle (\boldsymbol{\xi}^*(\boldsymbol{r}_1)\cdot \boldsymbol{S}(\boldsymbol{r}_1,t_1))\,(\boldsymbol{\xi}(\boldsymbol{r}_2)\cdot \boldsymbol{S}^*(\boldsymbol{r}_2,t_2))\rangle,\end{aligned} \tag{9}$$

[1] Linear terms are defined as the product of an equilibrium quantity and a fluctuating one.

where subscripts 1 and 2 denote two spatial and temporal locations. To proceed further, it is convenient to define the following coordinates:

$$\begin{aligned} \boldsymbol{x}_0 &= \frac{\boldsymbol{r}_2+\boldsymbol{r}_1}{2} \qquad t_0 = \frac{t_1+t_2}{2} \\ \boldsymbol{r} &= \boldsymbol{r}_2-\boldsymbol{r}_1 \qquad \tau = t_2-t_1 \end{aligned}$$

where $\boldsymbol{x}_0$ and t_0 are the average space-time position and $\boldsymbol{r}$ and τ are related to the local turbulence.

In the following, $\boldsymbol{\nabla}_0$ is the large-scale derivative associated with $\boldsymbol{x}_0$, $\boldsymbol{\nabla}_r$ is the small-scale one associated with $\boldsymbol{r}$, and the derivative operators $\boldsymbol{\nabla}_1$ and $\boldsymbol{\nabla}_2$ are associated with $\boldsymbol{r}_1$ and $\boldsymbol{r}_2$, respectively. The mean-squared amplitude can be rewritten in terms of the new coordinates as

$$\begin{aligned} \left\langle |\, A\,|^2\,(t)\right\rangle &= \frac{1}{4(\omega_0 I)^2} \\ &\times \int_{-\infty}^{t} \mathrm{d}t_0\, \mathrm{e}^{2\eta(t_0-t)} \int_{2(t_0-t)}^{2(t-t_0)} \mathrm{d}\tau \int \mathrm{d}^3x_0\, \mathrm{d}^3r\ \mathrm{e}^{-\mathrm{i}\omega_0\tau} \\ &\times \left\langle \left(\boldsymbol{\xi}^* \cdot \boldsymbol{\mathcal{S}}[\boldsymbol{x}_0-\frac{\boldsymbol{r}}{2}, t_0-\frac{\tau}{2}]\right)\left(\boldsymbol{\xi}\cdot\boldsymbol{\mathcal{S}}^*\left[\boldsymbol{x}_0+\frac{\boldsymbol{r}}{2}, t_0+\frac{\tau}{2}\right]\right)\right\rangle. \end{aligned} \quad (10)$$

Subscripts 1 and 2 are the values taken at the spatial and temporal positions $[\boldsymbol{x}_0-\frac{\boldsymbol{r}}{2}, -\frac{\tau}{2}]$ and $[\boldsymbol{x}_0+\frac{\boldsymbol{r}}{2}, \frac{\tau}{2}]$ respectively. In the excitation region, the eddy lifetime is much smaller than the oscillation lifetime ($\sim 1/\eta$) of p modes such that the integration over τ can be extended to infinity. Hence all time integrations over τ are understood to be performed over the range $]-\infty, +\infty[$.

We assume a stationary turbulence, therefore the source term (S) in Eq. (10) is invariant to translation in t_0. Integration over t_0 in Eq. (10) and using the definition of $\boldsymbol{S}$ (Eq. (6), Eqs. (7) and (8) yields

$$\langle |A|^2\rangle = \frac{1}{8\eta(\omega_0 I)^2}\left(C_{\mathrm{R}}^2 + C_{\mathrm{S}}^2 + C_{RS}\right), \quad (11)$$

where C_{R}^2 and C_{S}^2 are the turbulent Reynolds stress and entropy fluctuation contributions whose expressions are, respectively,

- the Reynolds source term:

$$\begin{aligned} C_{\mathrm{R}}^2 &= \int \mathrm{d}^3x_0 \int_{-\infty}^{+\infty} \mathrm{d}\tau\, \mathrm{e}^{-\mathrm{i}\omega_0\tau} \int \mathrm{d}^3r \\ &\times \left\langle \left(\rho_0\, u_j u_i\, \nabla_0^j \xi^i\right)' \left(\rho_0\, u_l u_m\, \nabla_0^l \xi^{*m}\right)''\right\rangle \end{aligned} \quad (12)$$

  where a *separation of scales* is assumed, i.e. that the spatial variation of the eigenfunctions is large compared to the typical length scale of turbulence (see Sect. 6 for a detailed discussion).
- the entropy contribution

$$\begin{aligned} C_{\mathrm{S}}^2 &= \int \mathrm{d}^3x_0 \int_{-\infty}^{+\infty} \mathrm{d}\tau\, \mathrm{e}^{-\mathrm{i}\omega_0\tau} \int \mathrm{d}^3r \\ &\times \left\langle \left(h_t\, \nabla_{0j}\xi^j\right)_1 \left(h_t\, \nabla_{0l}\xi^{*l}\right)_2 \right\rangle, \end{aligned} \quad (13)$$

where C_{RS} is the cross-source term representing interference between source terms. For p modes, C_{RS} turn out to be negligible because it involves third-order correlation products that are small and strictly vanish under the QNA assumption (Belkacem et al. 2006b).

2.1. Turbulent Reynolds stress contribution

Equation (12) is first rewritten as

$$\begin{aligned} C_{\mathrm{R}}^2 &= \int \mathrm{d}^3x_0 \int_{-\infty}^{+\infty} \mathrm{d}\tau\, \mathrm{e}^{-\mathrm{i}\omega_0\tau} \int \mathrm{d}^3r\, \rho_0^2 \\ &\times \nabla_0^j \xi^i \left\langle \left(u_j u_i\right)_1 (u_l u_m)_2 \right\rangle \nabla_0^l \xi^{*m}. \end{aligned} \quad (14)$$

The fourth-order moment is then approximated assuming the quasi-normal approximation (QNA, Lesieur 1997, Chap. VII-2) as in Paper I. The QNA is a convenient means of decomposing the fourth-order velocity correlations in terms of a product of second-order velocity correlations; that is, one uses

$$\begin{aligned} \langle (u_i u_j)_{(1)} (u_l u_m)_{(2)}\rangle &= \langle (u_i u_j)_{(1)}\rangle \langle (u_l u_m)_{(2)}\rangle \\ &+ \langle (u_i)_{(1)} (u_l)_{(2)}\rangle \langle (u_j)_{(1)} (u_m)_{(2)}\rangle \\ &+ \langle (u_i)_{(1)} (u_m)_{(2)}\rangle \langle (u_j)_{(1)} (u_l)_{(2)}\rangle. \end{aligned} \quad (15)$$

A better approximation is the closure model with plumes (Belkacem et al. 2006a,b) which can be adapted to the present formalism in order to take the presence of up and downdrafts in the solar convection zone into account.

It is then possible to express the Fourier transform (FT) of the resulting second-order moments in term of the turbulent kinetic and entropy energy spectrum (see Paper I for details)

$$\phi_{ij} = FT(\langle u_i u_j\rangle) = \frac{E(k,\omega)}{4\pi k^2}\left(\delta_{ij} - \frac{k_i k_j}{k^2}\right), \quad (16)$$

where $E(k,\omega)$ is the turbulent kinetic energy spectrum.

The turbulent Reynolds term Eq. (12) takes the following general expression under the assumption of isotropic turbulence:

$$C_{\mathrm{R}}^2 = \pi^2 \int \mathrm{d}^3x_0 \left(\rho_0^2\, b_{ij}^* b_{lm}\right) S_{(R)}^{ijlm}(\omega_0) \quad (17)$$

where

$$\begin{aligned} S_{(R)}^{ijlm} &= \int_{-\infty}^{+\infty} \mathrm{d}\omega \int \mathrm{d}^3k \left(T^{ijlm} + T^{ijml}\right) \\ &\times \frac{E^2(k)}{k^4} \chi_k(\omega_0+\omega)\chi_k(\omega) \end{aligned} \quad (18)$$

$$T^{ijlm} = \left(\delta^{il} - \frac{k^i k^l}{k^2}\right)\left(\delta^{jm} - \frac{k^j k^m}{k^2}\right) \quad (19)$$

$$b_{ij} \equiv \boldsymbol{e}_i \cdot (\boldsymbol{\nabla}_0 : \boldsymbol{\xi}) \cdot \boldsymbol{e}_j \quad (20)$$

where $\{\boldsymbol{e}_i\}$ are the spherical coordinate unit vectors, $(\boldsymbol{k},\omega)$ are the wavenumber and frequency associated with the turbulent eddies and turbulent kinetic energy spectrum $E(\boldsymbol{k},\omega)$, which is expressed as the product $E(\boldsymbol{k})\chi_k(\omega)$ for isotropic turbulence (Lesieur 1997). The kinetic energy spectrum $E(k)$ is normalized as

$$\int_0^\infty \mathrm{d}k\, E(k) = \frac{1}{2}\,\Phi w^2 \quad (21)$$

where w is an estimate for the vertical convective velocity and Φ is a factor introduced by Gough (1977) to take anisotropy effects into account. A detailed discussion of the temporal correlation function (χ_k) is addressed in Samadi et al. (2003b).

The contribution of the Reynolds stress can thus be written as (see Appendix A.1)

$$C_{\mathrm{R}}^2 = 4\pi^3 \int \mathrm{d}m\, \rho_0\, R(r)\, S_{\mathrm{R}}(\omega_0), \quad (22)$$

with

$$R(r) = \frac{16}{15}\left|\frac{\mathrm{d}\xi_r}{\mathrm{d}r}\right|^2 + \frac{44}{15}\left|\frac{\xi_r}{r}\right|^2 + \frac{4}{5}\left(\frac{\xi_r^*}{r}\frac{\mathrm{d}\xi_r}{\mathrm{d}r} + c.c\right) + L^2\left(\frac{11}{15}\,|\zeta_r|^2 - \frac{22}{15}(\frac{\xi_r^*\xi_h}{r^2} + c.c)\right) - \frac{2}{5}L^2\left(\frac{\mathrm{d}\xi_r^*}{\mathrm{d}r}\frac{\xi_h}{r} + c.c\right) + \left|\frac{\xi_h}{r}\right|^2\left(\frac{16}{15}L^4 + \frac{8}{5}\mathcal{F}_{\ell,|m|} - \frac{2}{3}L^2\right) \quad (23)$$

where we have defined

$$L^2 = \ell(\ell+1) \quad (24)$$

$$\zeta_r \equiv \frac{\mathrm{d}\xi_h}{\mathrm{d}r} + \frac{1}{r}(\xi_r - \xi_h) \quad (25)$$

$$\mathcal{F}_{\ell,|m|} = \frac{|m|(2\ell+1)}{2}\Big(\ell(\ell+1) - (m^2+1)\Big) \quad (26)$$

$$S_{\mathrm{R}}(\omega_0) = \int \frac{\mathrm{d}k}{k^2}\,E^2(k)\int \mathrm{d}\omega\,\chi_k(\omega+\omega_0)\,\chi_k(\omega). \quad (27)$$

Note that in the present work, nonradial effects are taken only into account through Eq. (23). A more complete description would require including anisotropic turbulence effects in Eq. (18), but this is beyond the scope of the present paper.

2.2. Entropy fluctuations contribution

The entropy source term is computed as for the Reynolds contribution in Sect. 2.1. Then Eq. (13) becomes

$$C_{\mathrm{S}}^2 = \frac{2\pi^2}{\omega_0^2}\int \mathrm{d}^3x_0\,\alpha_{\mathrm{s}}^2\,h^{ij}\,S_{ij}^{(S)}(\omega_0)\,, \quad (28)$$

where

$$S_{ij}^{S}(\omega_0) = \int \mathrm{d}^3k\,T_{ij}\,\frac{E(k)}{k^2}\,\frac{E_{\mathrm{s}}(k)}{k^2}\int \mathrm{d}\omega\,\chi_k(\omega_0+\omega)\chi_k(\omega)$$

with

$$T_{ij} = \left(\delta_{ij} - \frac{k_ik_j}{k^2}\right), \quad (29)$$

where $E_{\mathrm{s}}(k)$ is the entropy spectrum (see Paper I), and

$$h^{ij} = |C|^2\,\nabla_1^i(\ln|\alpha_{\mathrm{s}}|)\,\nabla_2^j(\ln|\alpha_{\mathrm{s}}|) - C^*\,\nabla_1^i(\ln|\alpha_{\mathrm{s}}|)\,\nabla_2^j(C) - C\,\nabla_1^i(\ln|\alpha_{\mathrm{s}}|)\,\nabla_2^j(C^*) + \nabla_1^i(C^*)\,\nabla_2^j(C)\,, \quad (30)$$

where $C \equiv \nabla.\boldsymbol{\xi}$ is the mode compressibility.

The final expression for the contribution of entropy fluctuations reduces to (see Appendix A.2)

$$C_{\mathrm{S}}^2 = \frac{4\pi^3\mathcal{H}}{\omega_0^2}\int \mathrm{d}^3x_0\,\alpha_{\mathrm{s}}^2\,(A_\ell + B_\ell)\,\mathcal{S}_{\mathrm{S}}(\omega_0), \quad (31)$$

where $\mathcal{H}$ is the anisotropy factor introduced in Paper I which, in the current assumption (isotropic turbulence), is equal to 4/3. In addition,

$$A_\ell \equiv \frac{1}{r^2}\left|D_\ell\,\frac{\mathrm{d}\,(\ln|\alpha_{\mathrm{s}}|)}{\mathrm{d}\ln r} - \frac{\mathrm{d}D_\ell}{\mathrm{d}\ln r}\right|^2 \quad (32)$$

$$B_\ell \equiv \frac{1}{r^2}\,L^2\,|D_\ell|^2 \quad (33)$$

$$\mathcal{S}_{\mathrm{S}}(\omega_0) \equiv \int \frac{\mathrm{d}k}{k^4}\,E(k)\,E_{\mathrm{s}}(k)\int \mathrm{d}\omega\,\chi_k(\omega_0+\omega)\,\chi_k(\omega) \quad (34)$$

where

$$D_\ell(r,\ell) \equiv D_r - \frac{L^2}{r}\,\xi_h\,,\ D_r \equiv \frac{1}{r^2}\,\frac{\mathrm{d}}{\mathrm{d}r}\left(r^2\xi_r\right). \quad (35)$$

3. The radial case

We show in this section that we recover the results of Paper I providing that:

- we restrict ourselves to the radial case by setting $\ell = 0$ ($\xi_h = 0$), and
- we assume a plane-parallel atmosphere.

In the entropy source term (C_{S}^2), the mode compressibility for a radial mode becomes

$$C = -\frac{\delta\rho}{\rho} = \frac{1}{r^2}\,\frac{\mathrm{d}\left(r^2\,\xi_r\right)}{\mathrm{d}r}\,Y_{\ell,m} \quad (36)$$

and from Eqs. (32) and (33), one then has

$$A_{\ell=0} = \frac{1}{r^2}\left|D_r\frac{\mathrm{d}}{\mathrm{d}\ln r}\ln|\alpha_{\mathrm{s}}| - \frac{\mathrm{d}D_r}{\mathrm{d}\ln r}\right|^2 \quad (37)$$

$$B_{\ell=0} = 0. \quad (38)$$

We thus obtain (Eq. (31))

$$C_{\mathrm{S}}^2 = \frac{4\pi^3\mathcal{H}}{\omega_0^2}\int \mathrm{d}^3x_0\,\alpha_{\mathrm{s}}^2 \times \frac{1}{r^2}\left|D_r\frac{\mathrm{d}\ln|\alpha_{\mathrm{s}}|}{\mathrm{d}\ln r} - \frac{\mathrm{d}D_r}{\mathrm{d}\ln r}\right|^2\,\mathcal{S}_{\mathrm{S}}(\omega_0). \quad (39)$$

For the Reynolds stress contribution, Eq. (22) reduces to

$$C_{\mathrm{R}}^2 = 4\pi^3\int \mathrm{d}^3x_0\,\rho_0^2 \times\left(\frac{16}{15}\left|\frac{\mathrm{d}\xi_r}{\mathrm{d}r}\right|^2 + \frac{44}{15}\left|\frac{\xi_r}{r}\right|^2 + \frac{4}{5}\frac{\xi_r^*}{r}\,\frac{\mathrm{d}\xi_r}{\mathrm{d}r} + c.c.\right)\mathcal{S}_{\mathrm{R}}(\omega_0). \quad (40)$$

To proceed further, we use the plane-parallel approximation. It is justified (for p modes) by the fact that excitation takes place in the uppermost part of the convection zone ($r/R \approx 1$). It is valid when the condition $r\,k_{\mathrm{osc}} \gg 1$ is fulfilled in the excitation region (k_{osc} being the local wavenumber), i.e. where excitation is dominant. Consequently,

$$\left|\frac{\mathrm{d}\xi_r}{\mathrm{d}r}\right| \gg \left|\frac{\xi_r}{r}\right|. \quad (41)$$

The validity of this inequality has been numerically verified and is discussed in Sect. 4 (Eq. (49))

With Eqs. (41), (39) and (40) simplify as

$$C_{\mathrm{S}}^2 = \frac{4\pi^3\mathcal{H}}{\omega_0^2}\int \mathrm{d}^3x_0\,\alpha_{\mathrm{s}}^2 \times \frac{1}{r^2}\left|\frac{\mathrm{d}\xi_r}{\mathrm{d}r}\frac{\mathrm{d}\ln|\alpha_{\mathrm{s}}|}{\mathrm{d}\ln r} - \frac{\mathrm{d}}{\mathrm{d}\ln r}\left(\frac{\mathrm{d}\xi_r}{\mathrm{d}r}\right)\right|^2\,\mathcal{S}_{\mathrm{S}}(\omega_0) \quad (42)$$

$$C_{\mathrm{R}}^2 = \frac{64}{15}\pi^3\int \mathrm{d}^3x_0\,\rho_0^2\left|\frac{\mathrm{d}\xi_r}{\mathrm{d}r}\right|^2\,\mathcal{S}_{\mathrm{R}}(\omega_0). \quad (43)$$

These are the expressions obtained by Paper I and Samadi et al. (2005) for the radial modes in a plane-parallel geometry.

4. Horizontal effects on the Reynolds and entropy source terms

We derive asymptotic expressions for the excitation source terms (Eqs. (22) and (31)) in order to identify the major nonradial contributors to the excitation rates in the solar case.

4.1. The ℓ dependence of the eigenfunctions

Let us consider the equation of continuity and the transverse component of the equation of motion for the oscillations. Let us neglect the Lagrangian pressure variation and Eulerian gravitational potential variation at $r = R$ (the surface). The ratio of the horizontal to the vertical displacement at the surface boundary is then approximately given by (Unno et al. 1989, p. 105)

$$\frac{\xi_h}{\xi_r} \simeq \sigma^{-2} , \tag{44}$$

where σ is the dimensionless frequency defined by

$$\sigma^2 = \frac{R^3}{GM}\omega^2 , \tag{45}$$

where ω is the angular frequency of the mode, R the star radius, and M its mass. Frequencies of solar p modes then range between $\sigma \approx 10$ and $\sigma \approx 50$ ($\nu \in [1, 5]$ mHz). Hence, for the solar oscillations, one always has

$$|\xi_r| \gg |\xi_h| . \tag{46}$$

However Eqs. (23) and (35) involve coefficients depending on the angular degree (ℓ). We then also consider the ratio

$$L^2\frac{\xi_h}{\xi_r} \approx L^2\,\sigma^{-2}. \tag{47}$$

Equation (47) is of order of unity for $\ell \sim \sigma$. For example, for a typical frequency of 3 mHz, one cannot neglect the horizontal effect $L^2\left|\frac{\xi_h}{r}\right|$ in front of $\left|\frac{\xi_r}{r}\right|$ for values of ℓ equal or greater than 30.

In what follows, we introduce the complex number f, which is the degree of non-adiabaticity, defined by the relation

$$f = \frac{\delta p/p}{\Gamma_1 \delta\rho/\rho}. \tag{48}$$

Note that $f = 1$ for adiabatic oscillations.

Let now compare the derivatives. Under the same assumptions above, neglecting the term in $(p/\rho)\mathrm{d}(\delta p/p)/\mathrm{d}r$ in the radial component of the equation of motion (standard mechanical boundary condition), one gets, near the surface,

$$\begin{aligned}\frac{\mathrm{d}\xi_r}{\mathrm{d}r}\Big/\left(\frac{\xi_r}{r}\right) &\simeq (f\Gamma_1)^{-1}[\sigma^2 + 2 + (L^2/\sigma^2 - 2)(f\Gamma_1 - 1)] \\ &\simeq \sigma^2/(f\Gamma_1).\end{aligned} \tag{49}$$

Hence, we always have $|\partial\xi_r/\partial r| \gg |\xi_r/r|$ in the excitation region (except near a node of $\partial\xi_r/\partial r$). Similar to Eq. (44), one can assume

$$\frac{\mathrm{d}\xi_h}{\mathrm{d}r}\Big/\frac{\mathrm{d}\xi_r}{\mathrm{d}r} \simeq \sigma^{-2} . \tag{50}$$

In fact, comparing Eq. (50) with the numerically-computed eigenfunctions shows that it holds even better than Eq. (44) in the excitation region.

Finally, we can group the different terms of Eqs. (23) and (31) into four sets

$$S_1 = \left|\frac{\mathrm{d}\xi_r}{\mathrm{d}r}\right|^2 \approx \sigma^4 \left|\frac{\xi_r}{r}\right|^2 , \tag{51}$$

$$S_2 = L^4\left|\frac{\xi_h}{r}\right|^2 \approx \frac{\ell^4}{\sigma^4}\left|\frac{\xi_r}{r}\right|^2 , \tag{52}$$

$$\begin{aligned}S_3 &= \left\{ L^2\left|\frac{\mathrm{d}\xi_r}{\mathrm{d}r}\right|\left|\frac{\xi_h}{r}\right|, L^2\left|\frac{\mathrm{d}\xi_h}{\mathrm{d}r}\right|^2 , L^2\left|\frac{\mathrm{d}\xi_h}{\mathrm{d}r}\right|\left|\frac{\xi_r}{r}\right|\right\} \\ &\approx \ell^2\left|\frac{\xi_r}{r}\right|^2 ,\end{aligned} \tag{53}$$

$$S_4 = \left\{ \left|\frac{\xi_r}{r}\right|^2 , \left|\frac{1}{r}\frac{\mathrm{d}|\xi_r|^2}{\mathrm{d}r}\right|, L^2\left|\frac{\xi_r}{r}\right|\left|\frac{\xi_h}{r}\right| \right\}. \tag{54}$$

The terms in S_4 are always negligible compared to the others. At fixed frequency (σ) we have thus:

$$S_1 \gg S_3 \gg S_4 \gg S_2 \text{ for } \ell \ll \sigma \tag{55}$$

$$S_1 \gg S_3 \gg S_4 \approx S_2 \text{ for } \ell \approx \sigma \tag{56}$$

$$S_1 \approx S_3 \approx S_2 \gg S_4 \text{ for } \ell \approx \sigma^2 \tag{57}$$

$$S_2 \gg S_3 \gg S_1 \gg S_4 \text{ for } \ell \gg \sigma^2. \tag{58}$$

In conclusion, the contribution of the horizontal displacement terms (S_2, S_3) begins to dominate the excitation for $\ell \gg \sigma^2$.

4.2. Source terms as functions of ℓ

Reynolds stress contribution:

We start by isolating non-radial effects in the range $\ell \in [0; 500]$. Note that the limit $\ell = 500$ is justified in Sect. 6.1 by the limit of validity for the present formalism. We investigate two cases, $\ell \ll \sigma^2$ and $\ell \approx \sigma^2$ respectively. The condition for which $\ell \simeq \sigma^2$ is satisfied for around the f mode for $\ell > 50$ and in the gap between the g_1 and f mode, for $\ell < 50$.

Using the set of inequalities Eqs. (55) to (58), for a typical frequency of 3 mHz (i.e. $\sigma \approx 30$), $R(r)$ (Eq. 23) becomes for high-n modes ($\ell \ll \sigma^2$):

$$R(r) \approx \frac{16}{15}\left|\frac{\mathrm{d}\xi_r}{\mathrm{d}r}\right|^2 . \tag{59}$$

Hence, for high-n acoustic modes one can use Eq. (59) instead of Eq. (23), and in terms of the excitation source term, the formalism reduces to the radial case for $\ell < 500$ and high-n modes.

For low-n modes ($\ell \approx \sigma^2$, i.e. for instance $\sigma \approx 10$) some additional dependency must be retained (see Eq. (57)). One gets

$$\begin{aligned}R(r) \approx\ & \frac{16}{15}\left|\frac{\mathrm{d}\xi_r}{\mathrm{d}r}\right|^2 + \frac{16}{15}L^4\left|\frac{\xi_h}{r}\right|^2 - \frac{2}{5}L^2\left(\frac{\mathrm{d}\xi_r^*}{\mathrm{d}r}\frac{\xi_h}{r} + c.c\right) \\ &+ \frac{11}{15}L^2\,|\zeta_r|^2 .\end{aligned} \tag{60}$$

The additional terms correspond to the non-diagonal contributions of the tensor $\boldsymbol{\nabla} : \boldsymbol{\xi}$ appearing in the Reynolds stress term C_{R}^2 because we are in the range $\ell \approx \sigma^2$ (see Eq. (57)). The radial and transverse components of the divergence of the displacement nearly cancel so that $\delta\rho/\rho$ takes its minimum values. This is due to the fact that they are nearly divergence-free, i.e.

$$\boldsymbol{\nabla}\cdot\boldsymbol{\xi} = D_\ell\, Y_\ell^m \approx \frac{\mathrm{d}\xi_r}{\mathrm{d}r} - L^2\frac{\xi_h}{r} \approx 0 . \tag{61}$$

As the divergence of the mode corresponds to the diagonal part of the tensor $\boldsymbol{\nabla} : \boldsymbol{\xi}$, one can then expect that the excitation rate decreases (through the terms in $\mathrm{d}\xi_r^*/\mathrm{d}r \times \xi_h/r$ in Eq. (60)). However, such a decrease is compensated for by the non-radial component of the tensor (ζ_r^2 in Eq. (60)). Thus, for low-n p modes there is a balance between the effect of incompressibility that tends to diminish the efficiency of the excitation and the non-diagonal components of the tensor $\boldsymbol{\nabla} : \boldsymbol{\xi}$ that tend to increase it.

Entropy contribution:

Numerical investigation shows that the non-radial component of the entropy source term does not affect the excitation rates significantly except for $\ell > 1000$, which is out of the validity domain of the present formalism (see Sect. 6.1). The non-radial effects appear through the mode compressibility, $L^2\,|D_\ell|^2$ (Eq. (33)). From Eq. (57) one can show that non-radial contributions play a non-negligeable role for low-n modes. However, such low-frequency modes are not enough localised in the superadiabatic zone, where the entropy source term is maximum, to be efficiently excited by this contribution.

5. Numerical estimations for a solar model

5.1. Computation of the theoretical excitation rates

In the following, we compute the excitation rates of p modes for a solar model. The rate (P) at which energy is injected into a mode per unit time is calculated according to the set of Eqs. (11)–(13). The calculation thus requires knowledge of four different types of quantities:

1) Quantities related to the oscillation modes: the eigenfunctions (ξ_r, ξ_h) and associated eigenfrequencies (ω_0).
2) Quantities related to the spatial and time-averaged properties of the medium: the density (ρ_0), the vertical velocity ($\tilde{w}$), the entropy ($\tilde{s}$), and $\alpha_\mathrm{s} = \partial P_1/\partial \tilde{s}$.
3) Quantities that contain information about spatial and temporal correlations of the convective fluctuations: $E(k)$, $E_\mathrm{s}(k)$, and $\chi_k(\omega)$.
4) A quantity that takes anisotropy into account: Φ measures the anisotropy of the turbulence and is defined according to Gough (1977) (see also Paper I for details) as:

$$\Phi = \frac{\langle u^2 \rangle}{\langle w^2 \rangle}, \tag{62}$$

where $u^2 = w^2 + u_h^2$ and u_h is the horizontal velocity.
To be consistent with the current assumption of isotropic turbulence, we assume $\Phi = 3$.

Eigenfrequencies and eigenfunctions (in point 1) above) were computed using the adiabatic pulsation code OSC (Boury et al. 1975). The solar structure model used for these computations (quantities in point 2) was obtained using the stellar evolution code CESAM (Morel 1997) for the interior, and a Kurucz (1993) model for the atmosphere. The interior-atmosphere match point was chosen at $\log\tau = 0.1$ (above the convective envelope). The pulsation computations used the full model (interior+ atmosphere). In the interior model, we used the OPAL opacities (Iglesias & Rogers 1996) extended to low temperatures with the opacities of Alexander & Ferguson (1994), and the CEFF equation of state (Christensen-Dalsgaard & Daeppen 1992). Convection is included according to a Böhm-Vitense mixing-length formalism (see Samadi et al. 2006, for details), from which $\tilde{w}$ is computed. The Φ value is set to 2 in the calculation. This is not completely consistent as we assume isotropic turbulence (i.e. $\Phi = 3$). This does not, however, affect the conclusions of the present paper, as all results on nonradial excitation rates are normalized to the radial ones. Note also that the equilibrium model does not include turbulent pressure. These two limitations are of small importance here as our investigation in this first work on nonradial modes remains essentially qualitative.

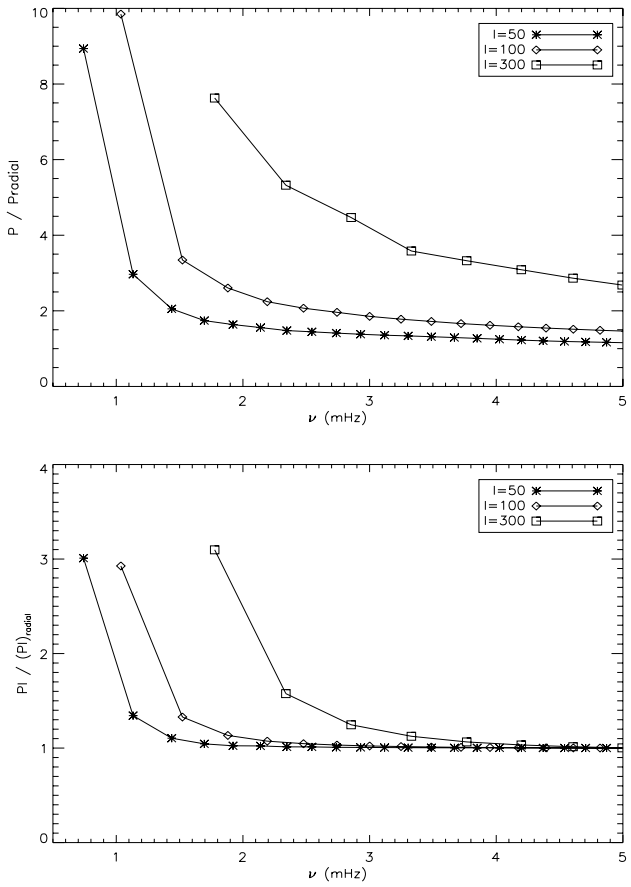

Fig. 1. *Top*: the rate (P) at which energy is supplied to each ℓ, n mode for $\ell = 50, 100, 300$ is divided by the excitation rate (P_radial) obtained for the $\ell = 0, n$ mode. Computation of the theoretical excitation rates is performed as explained in Sect. 5.1. *Bottom*: ratio $P\,I/(P\,I)_\mathrm{radial}$ where I is the mode inertia.

Finally, for the quantities in point 3, the total kinetic energy contained in the turbulent kinetic spectrum ($E(k)$) is obtained following Samadi et al. (2006).

5.2. Excitation rates

The rate (P) at which energy is supplied to the modes is plotted in Fig. 1, normalized to the radial excitation rate (P_rad). It is seen that the higher the ℓ, the more energy is supplied to the mode. This is explained by additional contributions (compared to the radial case) due to mode inertia, the spherical symmetry (departure from the plane-parallel assumption), and the contribution of horizontal excitation. Note that, as discussed in Sect. 3 (see Eq. (41)), the departure from the plane-parallel

approximation is negligible for p modes. Then, to discuss the other two contributions, one can rewrite Eq. (4) as

$$P = \left(\frac{|\xi_r(R)|^2}{8I}\right) \times \left(\frac{C_{\rm R}^2 + C_{\rm S}^2}{|\xi_r(R)|^2}\right), \tag{63}$$

where $|\xi_r(R)|$ is taken at the photosphere. Note that both terms of the product (Eq. (63)) are independent of the normalization of the eigenfunctions. Thus, as shown by Eq. (63), the power supplied to the modes is composed of two contributions that both depend on ℓ. The first is due to the mode inertia, which is defined as

$$I = \int_0^M {\rm d}m\ |\boldsymbol{\xi}|^2 = \int_0^R \left(|\xi_r|^2 + L^2\,|\xi_h|^2\right) r^2\,\rho_0 {\rm d}r. \tag{64}$$

High-ℓ modes present a lower inertia despite the L^2 contribution in Eq. (64) because they are confined high in the atmosphere where the density is lower than in deeper layers.

The second term of the product Eq. (63) depends on the non-radial effects through the excitation source terms (Eqs. (31) and (22)). To investigate this quantity independent of the mode mass (defined as $I/\,|\xi_r(R)|^2$), we plot the ratio $PI/(PI)_{\rm radial}$ in Fig. 1. One can then discuss two types of modes, namely low-n (≤ 3) and high-n (>3) modes (see Fig. 1).

- For high-n modes, non-radial effects play a minor role in the excitation source terms. The dominant effect (see Fig. 1) is due to the mode inertia as discussed above.
- For lower values of n, there is a contribution to the excitation rates due to the horizontal terms in Eq. (22).

Thus, contrary to high-n modes, the term $\frac{{\rm d}\xi_r}{{\rm d}r}$ in $R(r)$ (Eq. (23)) is no longer dominant in front of the terms involving ξ_h for low-order modes. Turbulence then supplies more energy to the low-frequency modes due to horizontal contributions, which explains the higher excitation rates for low-n modes as seen in Fig. 1. We stress that there is still turbulent energy that is supplied to the modes despite their nearly divergence-free nature. For such modes, the non-diagonal part of the tensor $\boldsymbol{\nabla} : \boldsymbol{\xi}$, which is related to the shear of the mode, compensates for and dominates the diagonal part, which is related to the mode compression.

5.3. Surface velocities

Another quantity of interest is the theoretical surface velocity, which can be compared to observational data. We compute the mean-squared surface velocity for each mode according to the relation (Baudin et al. 2005):

$$v_{\rm s}^2(\omega_0) = \frac{P(\omega_0)}{2\,\pi\,\Gamma_\nu\,\mathcal{M}} \tag{65}$$

where $\mathcal{M} \equiv I/\xi_{\rm r}^2(h)$ is the mode mass, h the height above the photosphere where oscillations are measured, $\Gamma_\nu = \eta/\pi$ the mode linewidth at half maximum (in Hz), and $v_{\rm s}^2$ is the mean square of the mode surface velocity. Equation (65) involves the damping rates ($\eta = \pi\Gamma_\nu$) inferred from observational data in the solar case for low-ℓ modes (see Baudin et al. 2005, for details). We then assume that the damping rates are roughly the same as for the $\ell = 0$ modes. Such an assumption is supported for low-ℓ modes ($\ell \approx 50$) as shown by Barban et al. (2004).

Figure 2 displays the surface velocities for $\ell = 0, 20$, and 50. Note that the surface velocities are normalized to the maximum velocity of the $\ell = 0$ modes ($V_0 \approx 8.5$ cm s^{-1} using MLT). This choice is motivated by the dependence of the absolute values of velocities on the convective model that is used, and it is certainly imperfect. However, its influence disappears when considering differential effects. As an indication, 3 σ error bars estimated from GOLF for the $\ell = 0$ modes are plotted (see Baudin et al. 2005, for details). The differences between the radial and non-radial computations are indeed larger than the $\ell = 0$ uncertainties for $\ell > 20$. For a more significant comparison, error bars for non-radial modes should be used, but they are difficult to determine with confidence (work in progress). For ℓ larger than 50, we do not give surface velocities; as derived, those here depend on the assumption of approximately constant damping rate that is not confirmed for $\ell > 50$.

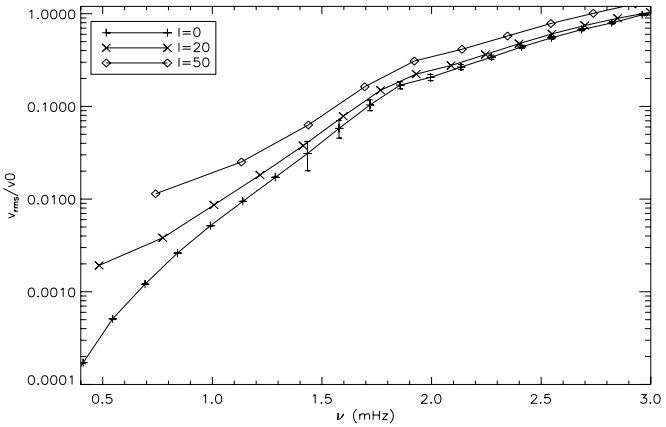

Fig. 2. Surface rms velocities of $\ell = 0, 20, 50$ modes calculated using Eq. (65) and normalized to the maximum velocity of the radial modes (see text). Note that the damping rates are taken from GOLF (Baudin et al. 2005) and are chosen to be the same for all angular degrees (ℓ). Three σ error bars derived from GOLF are plotted on the $\ell = 0$ curve.

When available, observational data should allow us to investigate the two regimes that have been emphasised in Sect. 5.2, namely the high- and low-n modes.

6. Discussion

6.1. The separation of scales

The main assumption in this general formalism appears in Eq. (11), where it has been assumed that the spatial variation of the eigenfunctions is large compared to the typical length scale of turbulence, leading to what we call *the separation of scales*. In order to test this assumption, one must compare the oscillation wavelength to the turbulent one or, equivalently, the wavenumbers. To this end, we use the dispersion relation (see Unno et al. 1989)

$$k_r^2 = \frac{\omega^2}{c_{\rm s}^2}\left(1 - \frac{S_\ell^2}{\omega^2}\right)\left(1 - \frac{N^2}{\omega^2}\right) \quad \text{and} \quad k_h^2 = \frac{L^2}{r^2} \tag{66}$$

where N is the buoyancy frequency, S_ℓ the Lamb frequency, and k_r, k_h the radial and horizontal oscillation wavenumbers, respectively, and $L^2 = \ell(\ell+1)$.

For the turbulent wavenumber, we choose to use, as a lower limit, the convective wavenumber $k_{\rm conv} = 2\pi/L_{\rm c}$, where $L_{\rm c}$ is the typical convective length scale. Thus, the assumption of separation of scales is fulfilled, provided

$$k_{r,h}/k_{\rm conv} \ll 1. \tag{67}$$

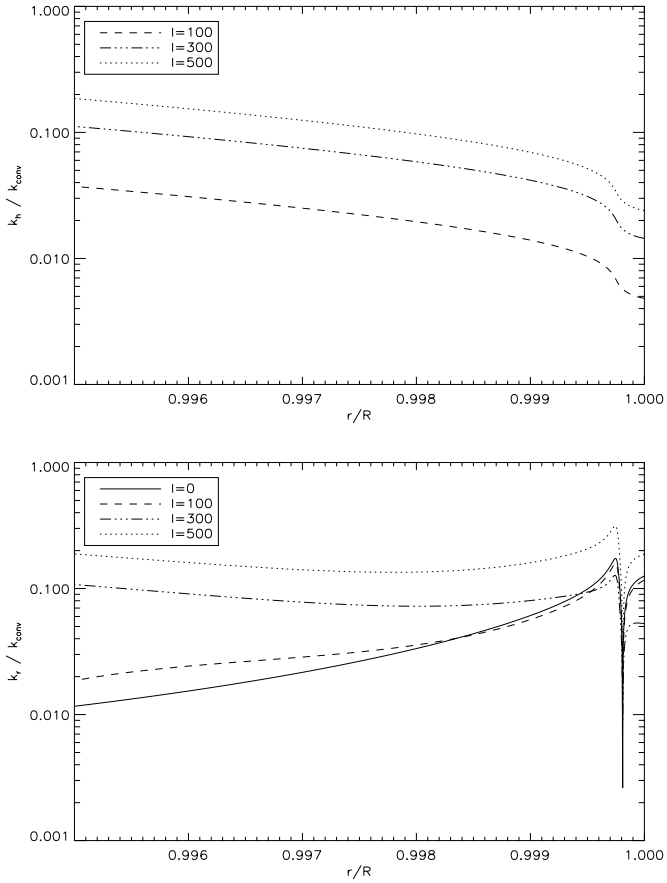

Fig. 3. *Top*: ratio of the horizontal oscillation wavenumber to the convective wavenumber ($k_h/k_{\rm conv}$), versus the normalized radius (r/R). $k_{\rm conv}$ is computed using the mixing length theory such that $k_{\rm conv} = 2\pi/L_{\rm c}$ ($L_{\rm c}$ is the mixing length) and k_r is computed using the dispersion relation Eq. (66). Note that the ratio $k_h/k_{\rm conv}$ is computed for a frequency of around $\nu = 3$ mHz, depending on the angular degree (ℓ). *Bottom*: the same as in the top but for the ratio $k_r/k_{\rm conv}$.

In Fig. 3 the ratios $k_r/k_{\rm conv}$ and $k_h/k_{\rm conv}$ are plotted. Those plots focus on the uppermost part of the solar convection zone where most of the excitation takes place. The assumption of separation of scale is valid for the horizontal component of the oscillation, since one has $k_h/k_{\rm conv} \ll 1$ (for $\ell \leq 500$) in the region where excitation is dominant. However, we must recall that our criterion is based on the mixing length for computing $k_{\rm conv}$. As shown by Samadi et al. (2003a) using 3D numerical simulations, the convective length scale (computed using the CESAM code, see Sect. 5.1) must be multiplied by a factor around five to reproduce the injection scale ($L_{\rm c}$) in the superadiabatic layers. Hence, for a more conservative criterion, we must then multiply the ratio $k_h/k_{\rm conv}$ by a factor of five, which leads to a ratio near unity for $\ell \approx 500$ (see Fig. 3). Thus, for higher values of the angular degree, the separation-of-scale hypothesis becomes doubtful.

Concerning the radial component of the oscillation wavenumber, the limiting value of ℓ seems to be the same (i.e. $\ell = 500$). Thus, we conclude that, for modes of angular degree lower than 500 one can use the separation of scales assumption. For $\ell > 500$, the characteristic length of the mode becomes shorter than the characteristic length $L_{\rm c}$ of the energy bearing eddies. Those modes will then be excited by turbulent eddies with a length-scale smaller than $L_{\rm c}$, i.e. lying in the turbulent cascade. These eddies inject less energy into the mode than the energy bearing eddies do, since they have less kinetic energy. We can then expect that – at fixed frequency – they received less energy from the turbulent eddies than the low-degree modes. A theoretical development is currently underway to properly treat the case of very high ℓ modes.

6.2. The closure model

A second approximation in the present formalism is the use of a closure model. The uppermost part of the convection zone is a turbulent convective system composed of two flows (upward and downward), and the probability distribution function of the fluctuations of the vertical velocity and temperature does not obey a Gaussian law (Lesieur 1997). Thus, the use of the quasi-normal approximation (QNA, Millionshchikov 1941), which is exact for a normal distribution, is no longer rigorously correct. A more realistic closure model has been developed in Belkacem et al. (2006a) and can be easily adapted for high-ℓ modes. This alternative approach takes the existence of two flows (the up- and downdrafts) within the convection zone into account. However, the QNA is nevertheless often used for the sake of simplicity as is the case here. Note that, when using the closure model with plumes, it is no longer consistent to assume that the third-order velocity moments strictly vanish; however, as shown by Belkacem et al. (2006a,b), their contribution is negligible in the sense that their effect is weaker than the accuracy of the presently available observational data.

6.3. Mode inertia

We have shown that the excitation rates for high-ℓ and n modes are sensitive to the variation in the mode inertia (I). The value of I depends on the structure of the stellar model and the properties of the eigenfunctions in these external regions. Samadi et al. (2006) have shown that different local formulations of convection can change the mode inertia by a small amount. This sensitivity then affects the computed excitation rates (P). However, the changes induced in P are found to be smaller than the accuracy to which the mode excitation rates are derived from the current observations (see Baudin et al. 2005; Belkacem et al. 2006b). Furthermore, concerning the way the modes are obtained, we have computed non-adiabatic eigenfunctions using the time-dependent formalism of Gabriel for convection (see Grigahcène et al. 2005). The mode inertia obtained with these non-adiabatic eigenfunctions exhibits a ν dependency different from those obtained using adiabatic eigenfunctions (the approximation adopted in the present paper). On the other hand, the mode inertia using non-adiabatic eigenfunctions (see Houdek et al. 1999, for details) obtained according to Gough's time-dependent formalism of convection (Gough 1977) shows smaller differences with the adiabatic mode inertia. Accordingly, the way the interaction of oscillation and time-dependent convection is modelled affects the eigenfunctions differently. As explained in Sect. 5.3, the formalism developed in this paper can be an efficient tool for deriving constraints on the mode inertia to distinguish between the different treatments of convection. Further work is thus needed on that issue.

7. Conclusions

We extended the Samadi & Goupil (2001) formalism in order to predict the amount of energy that is supplied to non-radial modes. In this paper, we focused on high-ℓ acoustic modes

with a particular emphasis on the solar case. The validity of the present formalism is limited to values of the angular degree lower than $\ell = 500$, due to the separation of scale assumption that is discussed above in Sect. 6.1. We have demonstrated that non-radial effects are due to two contributions, namely the effect of inertia that prevails for high-order modes ($n > 3$) and non-radial contributions in the Reynolds source term in $C^2_{\rm R}$ (see Eq. (22)) that dominate the radial one for low-order modes ($n < 3$).

Contrary to Belkacem et al. (2006b) who used 3D simulations to build an equilibrium model, we restricted ourselves to the use of a simple classical 1D MLT equilibrium model. Indeed, we were interested in deriving qualitative conclusions on nonradial contributions. Forthcoming quantitative studies will have to use more realistic equilibrium models, particularly for the convection description, such as models including turbulent pressure (e.g. Balmforth 1992) or patched models (e.g. Rosenthal et al. 1999).

From a theoretical point of view, several improvements and extensions of the present formalism remain to be carried out. For instance, one must relax the assumption of the separation of scales if one wants to model very high-ℓ modes. Such an investigation (which is currently underway) should enable us to draw conclusions about the observational evidence that, beyond some value of ℓ the energy supplied to the modes decreases with frequency (see Woodard et al. 2001, Fig. 2). Another hypothesis is the isotropic turbulence that has been assumed in the present work as a first approximation. Such an assumption needs to be given up to get a better description of the nonradial excitation of modes by turbulent convection, which requires further theoretical developments.

The present work focuses on p modes, but the formalism is valid for both p and g modes. We will address the analysis of gravity modes in a forthcoming paper.

Appendix A: Detailed expressions for source terms

The eigenfunctions ($\boldsymbol{\xi}$) are developed in spherical coordinates ($\boldsymbol{e}_r, \boldsymbol{e}_\theta, \boldsymbol{e}_\phi$) and expanded in spherical harmonics. Hence, the fluid displacement eigenfunction for a mode with given n, ℓ, m is written as

$$\boldsymbol{\xi}(\boldsymbol{r}) = (\xi_r \boldsymbol{e}_r + \xi_h \boldsymbol{\nabla}_H)\ Y_{\ell,m} \tag{A.1}$$

with

$$\boldsymbol{\nabla}_H = \begin{cases} \boldsymbol{e}_\theta \dfrac{\partial}{\partial\theta} \\ \boldsymbol{e}_\phi \dfrac{1}{\sin\theta}\dfrac{\partial}{\partial\phi} \end{cases} \tag{A.2}$$

where the spherical harmonics ($Y_{\ell,m}(\theta,\phi)$) are normalized according to

$$\int \frac{\mathrm{d}\Omega}{4\pi}\, Y_{\ell,m}\, Y^*_{\ell,m} = 1 \tag{A.3}$$

with Ω being the solid angle ($\mathrm{d}\Omega = \sin\theta\,\mathrm{d}\theta\mathrm{d}\phi$).
The large-scale gradient $\boldsymbol{\nabla}_0$ appearing in Eqs. (13) and (14) for instance is given, in the local spherical coordinates, by

$$\boldsymbol{\nabla}_0 = \boldsymbol{e}_r \frac{\partial}{\partial r} + \frac{1}{r}\boldsymbol{\nabla}_H\,. \tag{A.4}$$

A.1. Contribution of the turbulent Reynolds stress

The Reynolds stress contribution can be written as (see Sect. 2.1)

$$C^2_{\rm R} = \pi^2 \int \mathrm{d}^3x_0 \left(\rho_0^2\, b^*_{ij} b_{lm}\right) \int \mathrm{d}^3k \int \mathrm{d}\omega \times \left(T^{ijlm} + T^{ijml}\right) \frac{E^2(k)}{k^4}\, \chi_k(\omega_0+\omega)\,\chi_k(\omega) \tag{A.5}$$

where

$$T^{ijlm} = \left(\delta^{il} - \frac{k^i k^l}{k^2}\right)\left(\delta_{jm} - \frac{k^j k^m}{k^2}\right). \tag{A.6}$$

and

$$b_{ij} \equiv \boldsymbol{e}_i \cdot (\boldsymbol{\nabla}_0 : \boldsymbol{\xi}) \cdot \boldsymbol{e}_j \tag{A.7}$$

where the double dot denotes the tensor product.

We now consider the covariant ($\boldsymbol{a}^r, \boldsymbol{a}^\theta, \boldsymbol{a}^\phi$) and the contravariant ($\boldsymbol{a}_r, \boldsymbol{a}_\theta, \boldsymbol{a}_\phi$) natural base coordinates where the eigenfunction can be expanded:

$$\boldsymbol{\xi} = \hat{\xi}^k \boldsymbol{e}_k = q_k \boldsymbol{a}^k \qquad k = \{r,\theta,\phi\}. \tag{A.8}$$

The natural and physical coordinates are related to each other by

$$\boldsymbol{e}_i = \frac{1}{\sqrt{|g_{ii}|}}\boldsymbol{a}_i, \tag{A.9}$$

where g_{ij} is the metric tensor in spherical coordinates (see Table 6.5-1 in Korn & Korn 1968), i.e.,

$$\begin{aligned} &g_{rr} = 1, \quad g_{\theta\theta} = r^2, \quad g_{\phi\phi} = r^2\sin^2\theta\,, \\ &g_{ij} = 0 \quad \text{for} \quad i \neq j. \end{aligned} \tag{A.10}$$

Equation (A.7), with the help of Eq. (A.8), can then be developed in covariant coordinates

$$\begin{aligned} \boldsymbol{\nabla}_0 : \boldsymbol{\xi} = \boldsymbol{a}^i \frac{\partial \boldsymbol{\xi}}{\partial x^i} &= \boldsymbol{a}^i\,\boldsymbol{a}^j \left(\frac{\partial q_j}{\partial x^i}\right) + \boldsymbol{a}^i\, q_j \left(\frac{\partial \boldsymbol{a}^j}{\partial x^i}\right) \\ &= \boldsymbol{a}^i\,\boldsymbol{a}^j \left(\frac{\partial q_j}{\partial x^i}\right) - q_j\,\Gamma^j_{pi}\,\boldsymbol{a}^i\,\boldsymbol{a}^p \end{aligned} \tag{A.11}$$

where Γ^j_{pi} is the Christoffel three-index symbol of the second kind (Korn & Korn 1968). According to Eqs. (A.11) and (A.9), b_{ij} (Eq. (A.7)) can be written as

$$b_{ij} = \frac{1}{\sqrt{|g_{ii}\, g_{jj}|}}\left(\frac{\partial q_j}{\partial x^i} - q_p\,\Gamma^p_{ji}\right). \tag{A.12}$$

To proceed, one has to express Eq. (A.12) in terms of the physical coordinates ($\hat{\xi}^k$). With the help of Eqs. (A.8) and (A.9), we relate the covariant coordinates q_i to the physical (contravariant) components $\hat{\xi}^j$

$$q_j = \frac{g_{ij}}{\sqrt{|g_{jj}|}}\,\hat{\xi}^j, \tag{A.13}$$

where the component $\hat{\xi}^k$ are derived from Eq. (A.1)

$$\hat{\xi}^r = \xi_r Y_{\ell,m}; \quad \hat{\xi}^\theta = \xi_h \frac{\partial Y_{\ell,m}}{\partial\theta}; \quad \hat{\xi}^\phi = \xi_h \frac{1}{\sin\theta}\frac{\partial Y_{\ell,m}}{\partial\phi}\,. \tag{A.14}$$

Hence Eq. (A.12) becomes

$$
\begin{aligned}
b_{rr} &= \left(\frac{\mathrm{d}\xi_r}{\mathrm{d}r}\right) Y_{\ell,m} \\
b_{r\theta} &= \left(\frac{\mathrm{d}\xi_h}{\mathrm{d}r}\right) \frac{\partial Y_{\ell,m}}{\partial \theta} \\
b_{r\phi} &= \left(\frac{\mathrm{d}\xi_h}{\mathrm{d}r}\right) \frac{1}{\sin\theta} \frac{\partial Y_{\ell,m}}{\partial \phi} \\
b_{\theta r} &= \frac{1}{r}(\xi_r - \xi_h) \frac{\partial Y_{\ell,m}}{\partial \theta} \\
b_{\theta\theta} &= \frac{\xi_h}{r}\left(\frac{\partial^2 Y_{\ell,m}}{\partial \theta^2}\right) + \frac{\xi_r}{r} Y_{\ell,m} \\
b_{\theta\phi} &= b_{\phi\theta} = \frac{\xi_h}{r} \frac{\partial}{\partial \theta}\left[\frac{1}{\sin\theta} \frac{\partial Y_{\ell,m}}{\partial \phi}\right] \\
b_{\phi r} &= \frac{1}{r}(\xi_r - \xi_h) \frac{1}{\sin\theta} \frac{\partial Y_{\ell,m}}{\partial \phi} \\
b_{\phi\phi} &= \frac{\xi_r}{r} Y_{\ell,m} + \frac{\xi_h}{r}\left[\frac{1}{\sin^2\theta}\left(\frac{\partial^2 Y_{\ell,m}}{\partial \phi^2}\right) + \frac{\cos\theta}{\sin\theta}\left(\frac{\partial Y_{\ell,m}}{\partial \theta}\right)\right].
\end{aligned}
\tag{A.15}
$$

The contribution of the Reynolds stress can thus be written as

$$
\begin{aligned}
C_{\mathrm{R}}^2 &= 4\pi^3 \int \mathrm{d}m \int \mathrm{d}k \int \mathrm{d}\omega \; R(r,k) \\
&\times \frac{E^2(k)}{k^2} \chi_k(\omega+\omega_0)\chi_k(\omega) \,,
\end{aligned}
\tag{A.16}
$$

where we have defined $\mathrm{d}m = 4\pi r^2 \rho_0 \mathrm{d}r$, and

$$
R(r,k) \equiv \int \frac{\mathrm{d}\Omega}{4\pi} \int \frac{\mathrm{d}\Omega_k}{4\pi} \, b_{ij}^* \, b_{lm} \left(T^{ijlm} + T^{ijml}\right) . \tag{A.17}
$$

Because $T^{ijlm} = T^{jiml}$, it is easy to show that

$$
R(r,k) \equiv \int \frac{\mathrm{d}\Omega}{4\pi} \int \frac{\mathrm{d}\Omega_k}{4\pi} \, B_{ij}^* \, B_{lm} \left(T^{ijlm} + T^{ijml}\right)
$$

where $B_{ij} \equiv (1/2)(b_{ij} + b_{ji})$.

Using the expression Eq. (A.6) for T^{ijlm}, we write

$$
R(r,k) \equiv R_1 - R_2 + R_3 \tag{A.18}
$$

where

$$
\begin{aligned}
R_1 &= 2 \int \frac{\mathrm{d}\Omega}{4\pi} \int \frac{\mathrm{d}\Omega_k}{4\pi} \left(\sum_{i,j} B_{ij}^* B_{ij}\right) \\
R_2 &= 4 \int \frac{\mathrm{d}\Omega}{4\pi} \int \frac{\mathrm{d}\Omega_k}{4\pi} \left(\sum_{i,j} B_{ij}^* B_{il} \frac{k_j k_l}{k^2}\right) \\
R_3 &= 2 \int \frac{\mathrm{d}\Omega}{4\pi} \int \frac{\mathrm{d}\Omega_k}{4\pi} \left(\sum_{i,j} B_{ij}^* B_{lm} \frac{k_i k_j k_l k_m}{k^4}\right) .
\end{aligned}
\tag{A.19}
$$

We assume isotropic turbulence, hence the $\boldsymbol{k}$ components satisfy

$$
\int \mathrm{d}\Omega_k \, \frac{k_i k_j}{k^2} = \delta_{ij} \int \mathrm{d}\Omega_k \, \frac{k_r^2}{k^2}
$$

with δ_{ij} as the Kronecker symbol for $i, j = r, \theta, \phi$. Then we obtain

$$
R_1 = 2 \int \frac{\mathrm{d}\Omega}{4\pi} \left(\sum_{i,j} |B_{ij}|^2\right)
$$

$$
\begin{aligned}
R_2 &= 4 \int \frac{\mathrm{d}\Omega}{4\pi} \int \frac{\mathrm{d}\Omega_k}{4\pi} \, \frac{k_r^2}{k^2} \left(\sum_{i,j} |B_{ij}|^2\right) = 2\alpha \, R_1 \\
R_3 &= 2\beta \int \frac{\mathrm{d}\Omega}{4\pi} \left(\sum_{i,j} |B_{ij}|^2 + \sum_{i\neq j} (B_{ii}^* B_{jj} + cc)\right) \\
&= \beta \, R_1 + 2\,\beta \left(\int \frac{\mathrm{d}\Omega}{4\pi} \sum_{i\neq j} \left(B_{ii}^* B_{jj} + c.c\right)\right),
\end{aligned}
\tag{A.20}
$$

where we have set

$$
\alpha \equiv \int \frac{\mathrm{d}\Omega_k}{4\pi} \, \frac{k_r^2}{k^2} \; ; \; \beta \equiv \int \frac{\mathrm{d}\Omega_k}{4\pi} \, \frac{k_r^4}{k^4} . \tag{A.21}
$$

To compute R_1, R_2, and R_3, we write

$$
\begin{aligned}
B_{rr} &= b_{rr}; B_{\theta\theta} = b_{\theta\theta}; B_{\phi\phi} = b_{\phi\phi} \\
B_{r\theta} &= \frac{1}{2} \, \zeta_r \frac{\partial Y_{\ell,m}}{\partial \theta} \\
B_{r\phi} &= \frac{1}{2} \, \zeta_r \frac{1}{\sin\theta} \frac{\partial Y_{\ell,m}}{\partial \phi} \\
B_{\theta\phi} &= b_{\theta\phi} = b_{\phi\theta}
\end{aligned}
\tag{A.22}
$$

with

$$
\zeta_r = \frac{\mathrm{d}\xi_h}{\mathrm{d}r} + \frac{1}{r}(\xi_r - \xi_h) \, . \tag{A.23}
$$

Using the expression Eq. (A.22) for the quantities B_{ij}, we obtain, after some manipulation,

$$
\begin{aligned}
R_1 &= 2\left|\frac{\mathrm{d}\xi_r}{\mathrm{d}r}\right|^2 + 4\left|\frac{\xi_r}{r}\right|^2 + 2L^2(L^2-1)\left|\frac{\xi_h}{r}\right|^2 \\
&\quad + L^2\left(|\zeta_r|^2 - 2\left(\frac{\xi_r^* \xi_h}{r^2} + c.c\right)\right).
\end{aligned}
\tag{A.24}
$$

For R_3, some lengthy manipulation leads to:

$$
\begin{aligned}
R_3/\beta &= 2\left|\frac{\mathrm{d}\xi_r}{\mathrm{d}r}\right|^2 + 8\left|\frac{\xi_r}{r}\right|^2 + 2\left(L^4 + 4\mathcal{F}_{\ell,|m|}\right)\left|\frac{\xi_h}{r}\right|^2 \\
&\quad + L^2\left(2\,|\zeta_r|^2 - 2\left(\frac{\mathrm{d}\xi_r^*}{\mathrm{d}r}\frac{\xi_h}{r} + 2\frac{\xi_r^* \xi_h}{r^2} + c.c\right)\right) \\
&\quad + 4\left(\frac{\xi_r^*}{r}\frac{\mathrm{d}\xi_r}{\mathrm{d}r} + c.c\right)
\end{aligned}
\tag{A.25}
$$

where we have defined

$$
\begin{aligned}
\mathcal{F}_{\ell,|m|} &= \frac{(2\ell+1)}{2} \\
&\quad \times \left((|m|+1)A_{\ell,|m|}^2 + (|m|-1)B_{\ell,|m|}^2\right)
\end{aligned}
\tag{A.26}
$$

$$
A_{\ell,m}^2 = \frac{1}{4}\left(\ell(\ell+1) - m(m+1)\right) \tag{A.27}
$$

$$
B_{\ell,m}^2 = \frac{1}{4}\left(\ell(\ell+1) - m(m-1)\right) . \tag{A.28}
$$

To derive R_1, R_2, and R_3, the following relations have been used

$$
\frac{\partial^2 Y_{\ell,m}}{\partial \theta^2} + \frac{\cos\theta}{\sin\theta} \frac{\partial Y_{\ell,m}}{\partial \theta} + \frac{1}{\sin^2\theta} \frac{\partial^2 Y_{\ell,m}}{\partial \phi^2} = -L^2 Y_{\ell,m} \tag{A.29}
$$

$$
-m\frac{\cos\theta}{sin\theta} Y_{\ell,m} = A_{\ell,m} Y_{\ell,m+1} \mathrm{e}^{-\mathrm{i}\phi} + B_{\ell,m} Y_{\ell,m-1} \mathrm{e}^{\mathrm{i}\phi} \tag{A.30}
$$

$$
\frac{\partial Y_{\ell,m}}{\partial \theta} = A_{\ell,m} Y_{\ell,m+1} \mathrm{e}^{-i\phi} - B_{\ell,m} Y_{\ell,m-1} \mathrm{e}^{\mathrm{i}\phi} \tag{A.31}
$$

$$\int \frac{\mathrm{d}\Omega}{4\pi} \left(\nabla_H Y^*_{\ell,m} \cdot \nabla_H Y_{\ell,m}\right) = L^2 \tag{A.32}$$

$$- \int \frac{\mathrm{d}\Omega}{4\pi} \left(\nabla^2_H Y^*_{\ell,m}\right) Y_{\ell,m} = L^2 \tag{A.33}$$

$$\int \frac{\mathrm{d}\Omega}{4\pi} \left|\partial_\theta\left(\frac{1}{sin\theta}\frac{\partial Y_{\ell,m}}{\partial\phi}\right)\right|^2 = \mathcal{F}_{\ell,|m|}\,. \tag{A.34}$$

Combining Eqs. (A.24), (A.20), (A.20), and (A.18), with $\alpha = 1/3, \beta = 1/5$ (isotropic turbulence, see Paper I for details), yields

$$\begin{aligned} R(r) = {} & \frac{16}{15}\left|\frac{\mathrm{d}\xi_r}{\mathrm{d}r}\right|^2 + \frac{44}{15}\left|\frac{\xi_r}{r}\right|^2 + \frac{4}{5}\frac{1}{r}\frac{\mathrm{d}|\xi_r|^2}{\mathrm{d}r} \\ & + L^2\left(\frac{11}{15}\,|\zeta_r|^2 - \frac{22}{15}\left(\frac{\xi_r^*\xi_h}{r^2} + c.c\right)\right) \\ & -\frac{2}{5}L^2\left(\frac{\mathrm{d}\xi_r^*}{\mathrm{d}r}\frac{\xi_h}{r} + c.c\right) \\ & + \left|\frac{\xi_h}{r}\right|^2\left(\frac{16}{15}L^4 + \frac{8}{5}\mathcal{F}_{\ell,m} - \frac{2}{3}L^2\right). \end{aligned} \tag{A.35}$$

For radial modes, this reduces to

$$R(r) = \frac{16}{15}\left|\frac{\mathrm{d}\xi_r}{\mathrm{d}r}\right|^2 + \frac{44}{15}\left|\frac{\xi_r}{r}\right|^2 + \frac{4}{5}\frac{\mathrm{d}\,|\xi_r|^2}{\mathrm{d}r}. \tag{A.36}$$

The final expression for the Reynolds source term is then given by

$$C^2_{\mathrm{R}} = 4\pi^3 \int \mathrm{d}m\;\; R(r)\, S_{\mathrm{R}}(\omega_0)\,, \tag{A.37}$$

with

$$S_{\mathrm{R}}(\omega_0) = \int \frac{\mathrm{d}k}{k^2}\, E^2(k) \int \mathrm{d}\omega\, \chi_k(\omega+\omega_0)\chi_k(\omega) \tag{A.38}$$

and $R(r)$ by Eq. (A.35).

A.2. Contribution of entropy fluctuations

We start from Eq. (28), and to proceed further in the derivation of the entropy fluctuation source term, one has to compute

$$\int \mathrm{d}\Omega_k\, h^{ij}\, T_{ij}\,. \tag{A.39}$$

Then, $\boldsymbol{\xi}$ and $\boldsymbol{k}$ are expanded in spherical coorindates $(\boldsymbol{a}_r, \boldsymbol{a}_\theta, \boldsymbol{a}_\phi)$. We assume an isotropic turbulence; as a consequence, the quantities $k_r\, k_\theta$, $k_r k_\phi$, $k_\theta k_\phi$ vanish when integrated over Ω_k. One next obtains

$$\int \mathrm{d}\Omega_k\, h^{ij}\, T_{ij} = 2\pi\,\mathcal{H}\,\left(h_{rr} + h_{\theta\theta} + h_{\phi\phi}\right) \tag{A.40}$$

where $\mathcal{H}$ is the anisotropy factor introduced in Paper I, which in the current assumption (isotropic turbulence) is equal to 4/3. Assuming that $\alpha_{\mathrm{s}} = \alpha_{\mathrm{s}}(r)$, we have, according to Eq. (A.4),

$$\begin{cases} h_{rr} = \left| C\,\dfrac{\mathrm{d}\ln|\,\alpha_{\mathrm{s}}\,|}{\mathrm{d}r} - \dfrac{\partial C}{\partial r}\right|^2 \\ h_{\theta\theta} = \dfrac{1}{r^2}\left|\dfrac{\partial C}{\partial\theta}\right|^2 \\ h_{\phi\phi} = \dfrac{1}{r^2\,\sin^2\theta}\left|\dfrac{\partial C}{\partial\phi}\right|^2. \end{cases} \tag{A.41}$$

To proceed, it is necessary to express the divergence of the eigenfunction

$$C \equiv \boldsymbol{\nabla}_0 \cdot \boldsymbol{\xi} = D_\ell\, Y^m_\ell \tag{A.42}$$

with

$$D_\ell(r,\ell) \equiv D_r - \frac{L^2}{r}\,\xi_h \;\;;\;\; D_r \equiv \frac{1}{r^2}\frac{\partial}{\partial r}\left(r^2\xi_r\right)\,, \tag{A.43}$$

where again $L^2 = \ell(\ell+1)$.
We next integrate Eq. (28) over $\mathrm{d}\Omega/4\pi$, the solid angle associated with the eigenfunctions $\boldsymbol{\xi}$. One obtains, with the help of Eq. (A.42) and according to Eq. (A.41),

$$\begin{aligned} & \int \frac{\mathrm{d}\Omega}{4\pi} \int \mathrm{d}\Omega_k\, h^{ij}\, T_{ij} = \\ & \frac{2\pi\mathcal{H}}{r^2}\left(L^2\,|D_\ell|^2 + \left|D_\ell\,\frac{\mathrm{d}\ln|\,\alpha_{\mathrm{s}}\,|}{\mathrm{d}\ln r} - \frac{\mathrm{d}D_\ell}{\mathrm{d}\ln r}\right|^2\right). \end{aligned} \tag{A.44}$$

The final expression for the contribution of entropy fluctuations reduces to

$$C^2_{\mathrm{S}} = \frac{4\pi^3\,\mathcal{H}}{\omega_0^2} \int \mathrm{d}^3x_0\,\alpha_{\mathrm{s}}^2\;(A_\ell + B_\ell)\;\mathcal{S}_{\mathrm{S}}(\omega_0), \tag{A.45}$$

where $\mathcal{H}$ is the anisotropy factor introduced in Paper I that in the current assumption (isotropic turbulence) is equal to 4/3. In addition,

$$A_\ell \equiv \frac{1}{r^2}\left|D_\ell\,\frac{\mathrm{d}\,(\ln|\,\alpha_{\mathrm{s}}\,|)}{\mathrm{d}\ln r} - \frac{\mathrm{d}D_\ell}{\mathrm{d}\ln r}\right|^2 \tag{A.46}$$

$$B_\ell \equiv \frac{1}{r^2}\,L^2\,|D_\ell|^2 \tag{A.47}$$

$$\begin{aligned} \mathcal{S}_{\mathrm{S}}(\omega_0) \equiv {} & \int \frac{\mathrm{d}k}{k^4}\,E(k)\,E_{\mathrm{s}}(k) \\ & \times \int \mathrm{d}\omega\,\chi_k(\omega_0+\omega)\,\chi_k(\omega)\,. \end{aligned} \tag{A.48}$$

References

Alexander, D. R., & Ferguson, J. W. 1994, ApJ, 437, 879
Balmforth, N. J. 1992, MNRAS, 255, 639
Barban, C., Hill, F., & Kras, S. 2004, ApJ, 602, 516
Baudin, F., Samadi, R., Goupil, M.-J., et al. 2005, A&A, 433, 349
Belkacem, K., Samadi, R., Goupil, M. J., & Kupka, F. 2006a, A&A, 460, 173
Belkacem, K., Samadi, R., Goupil, M. J., Kupka, F., & Baudin, F. 2006b, A&A, 460, 183
Boury, A., Gabriel, M., Noels, A., Scuflaire, R., & Ledoux, P. 1975, A&A, 41, 279
Christensen-Dalsgaard, J. 2002, Inter. J. Mod. Phys. D, 11, 995
Christensen-Dalsgaard, J. & Daeppen, W. 1992, A&ARv, 4, 267
Dintrans, B., Brandenburg, A., Nordlund, Å., & Stein, R. F. 2005, A&A, 438, 365
Goldreich, P., & Keeley, D. A. 1977, ApJ, 212, 243
Goldreich, P., Murray, N., & Kumar, P. 1994, ApJ, 424, 466
Gough, D. O. 1977, ApJ, 214, 196
Gough, D. O. 1985, Theory of Solar Oscillations, Tech. Rep.
Grigahcène, A., Dupret, M.-A., Gabriel, M., Garrido, R., & Scuflaire, R. 2005, A&A, 434, 1055
Houdek, G. 2006, [arXiv:astro-ph/0612024]
Houdek, G., Balmforth, N. J., Christensen-Dalsgaard, J., & Gough, D. O. 1999, A&A, 351, 582
Iglesias, C. A., & Rogers, F. J. 1996, ApJ, 464, 943
Korn, G. A., & Korn, T. M. 1968, Mathematical handbook for scientists and engineers. Definitions, theorems, and formulas for reference and review (New York: McGraw-Hill, 2nd enl. and rev. edition)
Korzennik, S. G., Rabello-Soares, M. C., & Schou, J. 2004, ApJ, 602, 481
Kumar, P., Quataert, E. J., & Bahcall, J. N. 1996, ApJ, 458, L83

Kurucz, R. 1993, ATLAS9 Stellar Atmosphere Programs and 2 km/s grid. Kurucz CD-ROM No. 13. Cambridge, Mass.: Smithsonian Astrophysical Observatory
Lesieur, M. 1997, Turbulence in Fluids (Kluwer Academic Publishers)
Millionshchikov, M. D. 1941, Doklady Acad. Nauk SSSR, 32, 611
Morel, P. 1997, A&AS, 124, 597
Rosenthal, C. S., Christensen-Dalsgaard, J., Nordlund, Å., Stein, R. F., & Trampedach, R. 1999, A&A, 351, 689
Samadi, R., & Goupil, M. . 2001, A&A, 370, 136
Samadi, R., Nordlund, Å., Stein, R. F., Goupil, M. J., & Roxburgh, I. 2003a, A&A, 404, 1129
Samadi, R., Nordlund, Å., Stein, R. F., Goupil, M. J., & Roxburgh, I. 2003b, A&A, 403, 303
Samadi, R., Goupil, M.-J., Alecian, E., et al. 2005, J. Astrophys. Atr., 26, 171
Samadi, R., Kupka, F., Goupil, M. J., Lebreton, Y., & van't Veer-Menneret, C. 2006, A&A, 445, 233
Stein, R., Georgobiani, D., Trampedach, R., Ludwig, H.-G., & Nordlund, Å. 2004, Sol. Phys., 220, 229
Stein, R. F., & Nordlund, Å. 2001, ApJ, 546, 585
Unno, W., Osaki, Y., Ando, H., Saio, H., & Shibahashi, H. 1989, Nonradial oscillations of stars (University of Tokyo Press, 2nd ed.)
Woodard, M. F., Korzennik, S. G., Rabello-Soares, M. C., et al. 2001, ApJ, 548, L103